

The impact of bubble diffusivity on confined oscillated bubbly liquid

Sergey Shklyaev¹ and Arthur V. Straube^{2,a)}

¹Department of Theoretical Physics, Perm State University, Bukirev 15, Perm 614990, Russia

²Institut für Theoretische Physik, Technische Universität Berlin, Hardenbergstr. 36, D-10623 Berlin, Germany and Department of Physics and Astronomy, University of Potsdam, Karl-Liebknecht-Str. 24/25, D-14476 Potsdam-Golm, Germany

(Received 25 November 2008; accepted 2 June 2009; published online 25 June 2009)

We consider the dynamics of monodisperse bubbly liquid confined by two plane solid walls and subject to small-amplitude high-frequency transverse oscillations. The period of these oscillations is assumed small in comparison with typical relaxation times for a single bubble but comparable with the period of volume eigenoscillations. The time-averaged description accounting for the two-way coupling between the liquid and the bubbles and for the diffusivity of bubbles is applied. We find nonuniform steady states with the liquid quiescent on average. At relatively low frequencies, accumulation of bubbles either at the walls or in planes parallel to the walls is detected. These one-dimensional states are shown to be unstable. At relatively high frequencies, this accumulation is found at the central plane and the solution is stable. © 2009 American Institute of Physics.

[DOI: 10.1063/1.3157237]

I. INTRODUCTION

The dynamics of single and multiple inclusions suspended in liquid medium has been attracting much attention for many years. Of special interest is bubbly medium with bubbles as soft, deformable objects. Because of their compressibility, bubbles are able to exhibit an additional “degree of freedom” if compared to solid, nondeformable inclusions. A simple example of the system where this factor becomes of crucial importance is bubbly liquid under high-frequency oscillations.

A well-known observation is the appearance of an averaged force on a single bubble suspended in the liquid under the action of acoustic field.¹⁻³ For instance, the time-averaged force exerted on the bubble of radius R in the standing wave of pressure $p=p_0(z)\cos\omega t$ is given by

$$\mathbf{F}_b = \frac{\pi R}{\rho\omega^2(\Omega^2 - 1)} \nabla p_0^2, \quad (1)$$

which in the particular case of $p_0(z)=P_0 \cos kz$ results in

$$\mathbf{F}_b = -\frac{\pi k R P_0^2}{\rho\omega^2(\Omega^2 - 1)} \sin(2kz) \mathbf{e}_z \quad (2)$$

with a nondimensional parameter

$$\Omega^2 = \frac{1}{\rho\omega^2 R^2} \left(3\gamma P_g - \frac{2\sigma}{R} \right), \quad (3)$$

where Ω presents the ratio of the eigenfrequency of volume oscillations^{4,5} to the frequency ω of external driving. Here, $k=\omega/c_0$ is the wave number, c_0 is the speed of sound in the liquid free of bubbles, P_g is the mean pressure in the bubble, ρ is the liquid density, σ is the surface tension, γ is the adiabatic exponent, and $\mathbf{e}_z=(0,0,1)$.

As follows from expression (2), the bubble moves to the antinodes of the pressure wave at low frequency ω ($\Omega > 1$) and to the nodes at high frequency ω ($\Omega < 1$). This generic behavior is known as the *primary Bjerknes effect* and the force as in Eq. (1) is referred to as the *Bjerknes force*.

The simplest approach to obtaining the averaged description of bubbly liquid is to treat the bubbles in a superimposed acoustic field individually, independent of each other.⁶ Each bubble in the field experiences the Bjerknes force. However, such description lacks in possible *collective* (or *feedback*) effects and may not work even for a very small concentration of bubbles. The point is that a collection of bubbles influences the ambient liquid so that eventually both phases can be firmly coupled, which is essential for the correct description. For instance, the presence of a small amount of bubbles is known to qualitatively change the propagation of acoustic wave in liquid.⁷ In the situation where the size of the bubble is small compared to the acoustic wavelength, the scattering by a single bubble is typically weak. However, an *ensemble of bubbles* is able to significantly scatter the wave because the bubbles coherently change their volume. In other words, in a liquid containing bubbles the speed of sound c_b can become much smaller than c_0 . If the acoustic wavelength is larger than the characteristic length L of the system, $c_0 \gg \omega L$, the pure liquid behaves as incompressible. At the same time, in the bubbly medium it may happen that $c_b \sim \omega L$ and therefore scattering effects become important.^{8,9}

The impact of feedback effects on the averaged dynamics of bubbly liquid has been addressed by Kobelev and Ostrovsky.¹⁰ They analyze a coupled problem of the averaged drift of bubbles and the scattering of acoustic wave by the bubbles. Such factors as polydispersity of the bubbly liquid, dissipation of bubble oscillations, and collisions of bubbles are taken into account. As a result, a generalized model of bubbly liquid is obtained. Not only do the bubbles follow the trajectories prescribed by the averaged force but their motion also modifies the acoustic field and hence,

^{a)}Author to whom correspondence should be addressed. Electronic mail: arthur.straube@gmail.com.

changes the averaged force. Particularly, propagation of a traveling acoustic wave in the semi-infinite liquid has been analyzed for two situations. A bubbly layer either of finite thickness or occupying the whole domain is considered. In the former case, the so-called effect of self-transparency is found.

Their study has been followed by a number of particular analyses based on similar approximations accounting for cavitation and diffusion of gas from the bubbles into the liquid.^{11–13} It has been shown that a spatially uniform state and a one-dimensional solitonlike solution turn out to be unstable. As a result of self-organization, an asymmetric state emerges.¹³

The essential point behind these studies^{10–13} is the assumption that the liquid is quiescent on average. Although this approximation may be ultimately justified in the cited works, its applicability is not guaranteed *a priori*. Generally, one should average the momentum equation for the liquid over time and then ascertain whether the full model admits the solution of interest. This procedure is to be followed even if one is interested in the basic state with the vanishing averaged flow. The first step in obtaining a consistent model that allows for the averaged flows has been recently performed in Ref. 14, Sec. IV. Both dissipation of the volume oscillation of the bubbles and bubble collisions are neglected. The frequency of vibrations is assumed to be so small that the liquid remains incompressible; the compressibility of the medium is caused solely by the bubbles.

The expression of the averaged volume force has been obtained for monodisperse bubbly liquid. The theory is applied to study evolution of the initially homogeneous bubbly liquid in a thin layer confined by solid walls and subject to transverse oscillations. Bubbles either accumulate in planes parallel to the walls or settle at the boundaries. This accumulation process leads to infinite growth of the concentration, which makes the description invalid at a certain moment of time. A more realistic picture corresponds to the saturation caused by dissipative processes, which have been ignored until now.

In the present paper we overcome this difficulty in the similar way we already applied for an incompressible suspension in the field of external force.¹⁵ We introduce diffusivity of bubbles, which naturally prevents the unphysical growth of the concentration and allows us to make a step beyond the previous findings. In Sec. II A, we formulate a theoretical model and in Sec. II B consider a possible mechanism leading to the effective bubble diffusivity. Section III focuses on the application of the proposed model to the analysis of quasiequilibrium states. The problem of stability is addressed in Sec. IV and the results are summarized in Sec. V.

II. PROBLEM STATEMENT

A. Basic assumptions and governing equations

Consider monodisperse bubbly liquid filling the space between two solid parallel planes separated by a distance $2h$. The system is subject to transverse harmonic oscillations of an amplitude a and a frequency ω . To apply the averaged

description developed earlier (see Ref. 14, Sec. IV), a number of requirements are to be satisfied. More precisely, we focus on a dilute bubbly liquid with the equilibrium radius of the bubble $R \ll h$. Despite the smallness of volume fraction of bubbles, $\phi \ll 1$, we describe the bubbles in terms of a *finite* field $\Phi \equiv \phi h^2 / R^2$, which is for simplicity referred to as the concentration. We consider small-amplitude and high-frequency oscillations in the sense that

$$ah \ll R^2, \quad \omega R^2 \gg \nu, \quad (4)$$

where ν is the kinematic viscosity of the liquid. For a detailed discussion of conditions that allow us to neglect dissipative processes for a single oscillating bubble, see Ref. 7.

On the other hand, the frequency ω is chosen so small that no acoustic waves are possible in the medium without bubbles, $\omega h \ll c_0$. As a result, at small Φ the carrier liquid moves like the solid body. As has been mentioned earlier, we are interested in the situation where the frequency of external driving is comparable with the eigenfrequency of the breathing mode. We choose the Cartesian reference frame with the origin located in the central plane of the layer. Axes x and y are aligned with the central plane and axis z is normal to the solid boundaries.

It has been shown before¹⁴ that under the above conditions a peaking regime occurs: The bubbles accumulate at certain planes, $z = \text{const}$, where their concentration grows abruptly to infinity within a finite time. As we announce in Sec. I, this unphysical growth can be remedied by introducing diffusion of bubbles. In Sec. II B, we support this idea by analyzing a possible mechanism of effective diffusivity of bubbles. The generalization of the averaged model for diffusive bubbles is straightforward. The principal point is that the presence of diffusion does not influence the pulsation problem and enters the averaged equations only. As a result, diffusion appears naturally in the flux of bubbles [see Eq. (5b)], as one intuitively expects.

By measuring the length, time, velocity, and pressure in the scales of h , $h^2 D^{-1}$, Dh^{-1} , and $\rho \nu D h^{-2}$, where D is the bubble diffusivity, we arrive at the dimensionless boundary value problem [cf. Eq. (52)–(55), Ref. 14],

$$\frac{1}{S} \left(\frac{\partial \mathbf{u}}{\partial t} + \mathbf{u} \cdot \nabla \mathbf{u} \right) = -\nabla p + \nabla^2 \mathbf{u} + 3Q_S \Phi_a \Phi \nabla \psi^2, \quad (5a)$$

$$\frac{\partial \Phi}{\partial t} + \text{div } \mathbf{j} = 0, \quad \mathbf{j} \equiv \mathbf{u}_b \Phi - \nabla \Phi, \quad (5b)$$

$$\text{div } \mathbf{u} = 0, \quad \mathbf{u}_b = \mathbf{u} + Q_S \nabla \psi^2, \quad (5c)$$

$$z = \pm 1: \quad \mathbf{u} = 0, \quad \mathbf{e}_z \cdot \mathbf{j} = 0. \quad (5d)$$

Here \mathbf{u} and \mathbf{u}_b are the velocities of the liquid and bubbles, respectively, p is the renormalized pressure, and \mathbf{j} is the flux of bubbles.

The amplitude ψ of the velocity potential of pulsation flow, which enters Eqs. (5a) and (5c), is determined by the boundary value problem [cf. Eqs. (44) and (45), Ref. 14],

$$\nabla^2 \psi + \frac{3\Phi_a \Phi(\mathbf{r})}{\Omega^2 - 1} \psi = 0, \quad (6a)$$

$$z = \pm 1: \quad \mathbf{e}_z \cdot \nabla \psi = 1. \quad (6b)$$

For the sake of brevity, hereafter ψ is called the velocity potential.

Boundary value problem (5) and (6) is governed by dimensionless parameters

$$Q_S = \frac{1}{4} \frac{a^2 \omega^2 h^2}{(\Omega^2 - 1) \nu D}, \quad S = \frac{\nu}{D}, \quad \Phi_a = \phi_a \frac{h^2}{R^2},$$

and Ω , given by expression (3). Here ϕ_a denotes the mean concentration of bubbles. The first parameter, Q_S , is proportional to the power of external driving. For this reason, hereafter we refer to $|Q_S|$ as the intensity of external driving. Parameter S is the Schmidt number, which is the ratio of the characteristic diffusion time to the viscous time scale. For most practically relevant situations S is high. The third parameter, Φ_a , stands for feedback, it presents a measure of how strongly the liquid motion is influenced by the bubbles (for a similar treatment of the particle feedback, see Ref. 15). Technically, this parameter serves as a scaling factor, it defines dimensionless concentration of the bubbles so that the space-averaged field Φ is normalized by unity. As introduced in Sec I, we distinguish below two opposite cases of low ($\Omega > 1$) and high ($\Omega < 1$) frequencies. It is important to note that this distinction is purely conventional and has no contradiction with the *high-frequency approximation* accepted for the averaged description.¹⁴ Generally, any value of Ω satisfies this approximation.

B. Physical interpretation of bubble diffusivity

In Sec. II A we phenomenologically introduced diffusivity of bubbles in the theoretical model. In this subsection we provide arguments that make such an approach physically sound. Although the natural diffusivity of bubbles is small, we point out a possible reason that can effectively enhance the process of spatial diffusion of bubbles. For the sake of convenience, we use dimensional variables throughout this section.

The analysis of the realistic situation implies taking into consideration a slight imperfection of the experimental setup. Dealing with a vibration process, we consider the shaker unit to be weakly noisy in the sense that the generated oscillations are not perfectly harmonic and transverse. Weak irregularity of the produced signal leads to spreading of the driving force spectrum. The field of liquid pulsation velocity, \mathbf{V} , is exerted through the boundaries and is therefore fluctuating. Note that despite such irregularity, this field must be irrotational. As a result, the fluctuation-modulated pulsation field can be presented as

$$\mathbf{V} = a\omega \nabla [\psi + \epsilon \zeta(\mathbf{r}, t)] \cos \omega t,$$

where $\zeta(\mathbf{r}, t)$ is a random function with the vanishing mean value and ϵ is the measure of the noise intensity, which is assumed small enough. Because of ergodicity, the averaging over realizations is equivalent to the time averaging at a fixed point of the system. Below we refer to this procedure as the “averaging over fluctuations.”

Generally speaking, to complete specification of the noise, the forms of the spatial and temporal correlations have to be prescribed. However, this is not necessary for providing estimations. The only essential point is to figure out the appropriate time and length scales.

We point out that the temporal variation of $\zeta(\mathbf{r}, t)$ takes place because of the mentioned spectrum spreading. The spatial variation of this field is assumed independent of the temporal one and can be caused by various reasons such as slight deviations from perfectly translational oscillatory motion of the boundaries, roughness of the boundaries confining the bubbly liquid, etc. According to these arguments, it is reasonable to assume that the typical time τ_s of the velocity modulation is large in comparison with the period of oscillations but small compared to the time scale of the averaged motion. The characteristic length scale r_s is larger than the bubble radius, R , but smaller than the system size, h . As a result, the temporal and spatial variations of $\zeta(\mathbf{r}, t)$ can be expected to satisfy inequalities

$$\omega^{-1} \ll \tau_s \ll h^2 \nu^{-1}, \quad (7)$$

$$R \ll r_s \ll h. \quad (8)$$

Hence, the correlation time and length can be estimated as $\tau_c = r_s^2 / \nu$ and $r_c = \sqrt{\nu \tau_s}$, respectively, which are easy to interpret. The time scale τ_c presents the typical viscous relaxation time of the velocity on the length scale r_s . The correlation length, r_c , can be thought of as the characteristic thickness of viscous boundary layer associated with an oscillatory process with the frequency τ_s^{-1} . This hierarchy of the characteristic times allows us to perform two successive time averagings: the first one over the period of oscillations and the next one over the fluctuations.

After the time averaging over the period of oscillations we obtain the Bjerknes force exerted on each bubble,

$$\mathbf{F}_b \sim \rho a^2 \omega^2 R \nabla (\psi^2 + 2\epsilon \psi \zeta),$$

if we assume $|\Omega^2 - 1| \approx 1$.

The first term is the usual primary Bjerknes force, whereas the second contribution presents a stochastic correction. Balancing this stochastic contribution with the Stokes force, one finds the stochastic correction to the bubble velocity

$$\mathbf{u}_s \sim \epsilon \frac{a^2 \omega^2}{\nu} \nabla (\psi \zeta),$$

which entails diffusion of a single bubble with an effective diffusion coefficient given by¹⁶

$$D = \langle u_s^2 \rangle \tau_c \sim \left[\frac{\epsilon (a \omega h)^2}{\nu r_s} \right]^2 \tau_c. \quad (9)$$

Here, the angle brackets denote the averaging over fluctuations. By recalling the definition of τ_c , we see that result (9) is formally independent of the scales τ_s and r_s . The existence of these scales and the fulfillment of requirements (7) and (8) are, however, important. The temporal variation of the velocity field \mathbf{u}_s ensures that each bubble diffuses in time. In view of the spatial variation of \mathbf{u}_s , the diffusive motion of bubbles

is spatially uncorrelated. For this reason, expression (9) defines the spatial diffusivity of bubbles in the liquid as was introduced in Sec. II A.

To make estimations, we choose the following values characterizing bubbly liquid and experimental conditions: $R \approx 3 \times 10^{-1}$ cm, $\nu \approx 10^{-2}$ cm² s⁻¹, $h \approx 10$ cm, $a \approx 10^{-3}$ cm, and $\omega \approx 10$ rad s⁻¹. We note that such choice satisfies theoretical requirements (4) and at the same time is in agreement with a typical vibration experiment, see, e.g., Ref. 17. For this set of parameters we can assign $\tau_s \approx 10$ s and $r_s \approx 1$ cm and then estimate $\tau_c \approx 10^2$ s and $r_c \approx 0.3$ cm. By letting the imperfection of the vibration signal be of order 1% ($\epsilon \sim 10^{-2}$) we end up with the effective diffusion $D \approx 10^{-2}$ cm² s⁻¹, which gives $|Q_S| \approx 10^2$. As we see, this diffusion process is significantly more intensive compared with the natural diffusivity, described by the coefficient $D_0 \approx 10^{-12}$ cm² s⁻¹, which has been evaluated for similar conditions at room temperature. We emphasize that the value of Q_S can be varied by tuning the frequency ω . The increase of ω up to 10^2 rad s⁻¹ leads to $D \approx 1$ cm² s⁻¹ and consequently $|Q_S| \approx 1$. Finally, we emphasize that the effective diffusivity of bubbles is dependent on the experimental conditions and may be weaker than the values provided here. This circumstance, however, would lead to higher localization of the states obtained in Sec. III only, without qualitative changes of the corresponding solutions.

III. QUASIEQUILIBRIUM STATE

We now perform a one-dimensional analysis of a stationary solution in which all the fields are functions of the z -coordinate only. Although the averaged liquid velocity is vanishing, the pulsation velocity is nontrivial. For this reason, the solution can be referred to as a *quasiequilibrium state* or simply a quasiequilibrium. We note that the vibration ‘‘Bjerknes’’ force exerted on the bubbles does not vanish. However, in contrast to the previous nondiffusive study,¹⁴ this force is now compensated by the diffusive flux so that the total bubble flux \mathbf{j}_0 turns to zero.

As a result, Eqs. (5) and (6) are reduced and for the quasiequilibrium state, we obtain

$$\Phi'_0 = Q_S \Phi_0 (\psi_0^2)', \quad (10a)$$

$$\psi_0'' = -\frac{3\Phi_a}{\Omega^2 - 1} \Phi_0 \psi_0, \quad (10b)$$

$$z = \pm 1: \quad \psi_0' = 1. \quad (10c)$$

Here, primes denote derivatives with respect to z . A closer look at Eq. (10) allows us to figure out symmetry properties of the solution. Potential ψ_0 and concentration Φ_0 have to be odd and even functions of z , respectively. Hence, the boundary value problem (10) can be treated in half of the domain, say, $0 \leq z \leq 1$, with the boundary condition

$$z = 0: \quad \psi_0 = 0, \quad (11)$$

and the impermeability condition (10c) at $z=1$.

Next, Eq. (10a) is easily integrated to yield

$$\Phi_0 = C \exp(Q_S \psi_0^2), \quad (12)$$

where the constant C is defined by the requirement of mass conservation

$$C^{-1} = \int_0^1 \exp(Q_S \psi_0^2) dz. \quad (13)$$

Note that from solution (12) and symmetry condition (11) it follows that the concentration has a maximum at $z=0$ for $\Omega < 1$ ($Q_S < 0$) and a minimum in the opposite case, $\Omega > 1$ ($Q_S > 0$). This observation is in agreement with the well-known primary Bjerknes effect: The bubbles accumulate in the nodes of pressure (which in our consideration coincide with the nodes of the velocity potential) at high frequencies and escape from the nodes at low frequencies.

The substitution of solution (12) into Eq. (10b) leads to an ordinary nonlinear differential equation for the velocity potential

$$\psi_0'' = -\frac{3C\Phi_a}{\Omega^2 - 1} e^{Q_S \psi_0^2} \psi_0. \quad (14)$$

Accounting for relation (10a), we integrate Eq. (14) and obtain

$$(\psi_0')^2 = 1 + \frac{3C\Phi_a}{Q_S(\Omega^2 - 1)} (e^{Q_S \psi_m^2} - e^{Q_S \psi_0^2}), \quad (15)$$

where $\psi_m \equiv \psi_0(1)$ and the result satisfies boundary condition (10c).

Equations (14) and (15) can be thought of as the second Newton law and the energy conservation law for a mechanical particle with ψ_0 and z playing the roles of the coordinate and time, respectively. This observation does not imply, however, full mechanical analogy because we deal with the boundary value problem but not with the initial value problem as in mechanics. Although generally this problem can be solved only numerically, in a number of limiting cases we obtain analytical solutions.

A. Low frequencies

We first focus on the case of low frequencies, for which we introduce a parameter

$$\alpha^2 \equiv \frac{3\Phi_a}{\Omega^2 - 1}.$$

We start with the consideration of the limit of large Q_S , in which all the bubbles accumulate at certain planes $z=z_c$ or in other words form narrow bubbly screens. Outside these screens the liquid is almost free of bubbles. In such domains $\Phi_0=0$ and therefore the Helmholtz Eq. (14) [or Eq. (10b)] is reduced to the Laplace equation with a linear solution for ψ_0 .

For $\alpha^2 < 2$, the bubbles tend to approach the solid walls and accumulate so that no bubbly screens appear away from the wall. The corresponding outer solution describing the potential in the bulk is

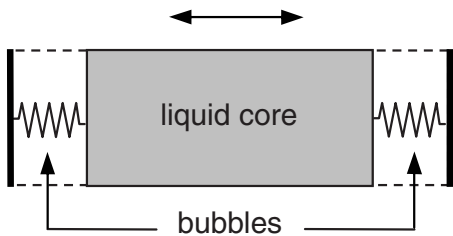


FIG. 1. Bubbly liquid as a resonator. At low frequencies bubbles localize near the walls and become equivalent to springs, while the liquid plays the role of the solid body.

$$\psi_0^{(o)} = \beta z, \quad \beta = \frac{1}{1 - \alpha^2}, \tag{16}$$

and consequently the concentration of bubbles is exponentially small. On the other hand, the inner solution, which describes the bubbly screens localized close to the walls, is given by the formulas

$$\Phi_0 = \frac{Q_S \beta (1 + \beta)}{F^2(\xi)}, \tag{17}$$

$$\psi_0^{(i)} = \beta - (\beta Q_S)^{-1} \ln F(\xi), \tag{18}$$

$$F = \cosh \beta^2 \xi + \beta^{-1} \sinh \beta^2 \xi, \tag{19}$$

where $\xi = Q_S(1 - z)$ is the “fast” coordinate near the wall.

Thus, the concentration Φ_0 is high near the walls. In contrast to the case of nondiffusive bubbles,¹⁴ the bubbles now cannot leave the system. As a result, the dynamics of liquid is strongly influenced by the bubbles. The carrier liquid moves as a solid body with the amplitude β , which is larger than the amplitude of external driving. The “air cushions” formed of bubbles near the walls are similar to springs (see Fig. 1) so that the altogether system acts as a resonator. Under periodic driving, the system displays forced oscillations with the resonant value $\alpha = 1$ ($\beta \rightarrow \infty$), which separates two qualitatively different regimes. At values $\alpha < 1$ ($\beta > 0$), the liquid at each point oscillates in phase with the walls. As follows from Eq. (19), function $F(\xi)$ is monotonic for positive β , and hence both the potential and the bubble concentration are maximal directly at the walls, see also Fig. 2(c). In the opposite case, $\alpha > 1$ ($\beta < 0$), the liquid core oscillates in counterphase with respect to the walls. Note that function

$F(\xi)$ is no longer monotonic. Thus, the concentration maximum is very close to the wall, but not exactly at the wall, Fig. 3(c). At the critical value $\alpha = 1$, resonant amplification of oscillation occurs. In this particular situation, even small dissipation must be taken into account.¹⁰

For $2 < \alpha^2 < 12$, the bubbly screen is localized at the point $z = z_1 \equiv 2\alpha^{-2}$. While far from this point the potential is a linear function

$$\psi_0^{(o)} = |z - z_1| - z_1, \tag{20}$$

the solution close to the screen can be described as

$$\Phi_0 = \frac{Q_S}{\alpha^2 \cosh^2 \xi}, \tag{21a}$$

$$\psi_0^{(i)} = -z_1 + (z_1 Q_S)^{-1} \ln \cosh \xi, \tag{21b}$$

with $\xi = (z - z_1)z_1 Q_S$.

At larger α^2 the number of bubbly screens increases. For $2n(2n - 1) < \alpha^2 < (2n + 1)(2n + 2)$ there exist n bubbly screens localized at

$$z = z_1 = 2n\alpha^{-2}, \quad z_2 = 3z_1, \dots, z_n = (2n - 1)z_1. \tag{22}$$

We note that in this case formulas (21) remain valid in the vicinity of bubbly screen k ($k = 1, \dots, n$), with $\xi_k = (z - z_k)z_1 Q_S$ and z_1 defined by Eq. (22). Another difference is that the sign of $\psi_0^{(i)}$ changes for even k .

We now proceed to the opposite limiting case of small Q_S , which is described by an asymptotic solution

$$\psi_0 = \psi_0^{(0)} + Q_S \psi_0^{(1)}, \quad \Phi_0 = 1 + Q_S \Phi_0^{(1)}, \tag{23a}$$

$$\psi_0^{(0)} = \frac{\sin \alpha z}{\alpha \cos \alpha}, \quad \Phi_0^{(1)} = \psi_0^2 + C_1, \tag{23b}$$

$$C_1 = \frac{\sin 2\alpha - 2\alpha}{4\alpha^3 \cos^2 \alpha} \quad (C = 1 + Q_S C_1), \tag{23c}$$

where

$$\psi_0^{(1)} = f_0 [z \cos \alpha z - (\cos \alpha - \alpha \sin \alpha) \psi_0^{(0)}] - \frac{1}{32\alpha^3 \cos^3 \alpha} [\sin 3\alpha z - 3\alpha \cos 3\alpha \psi_0^{(0)}], \tag{24}$$

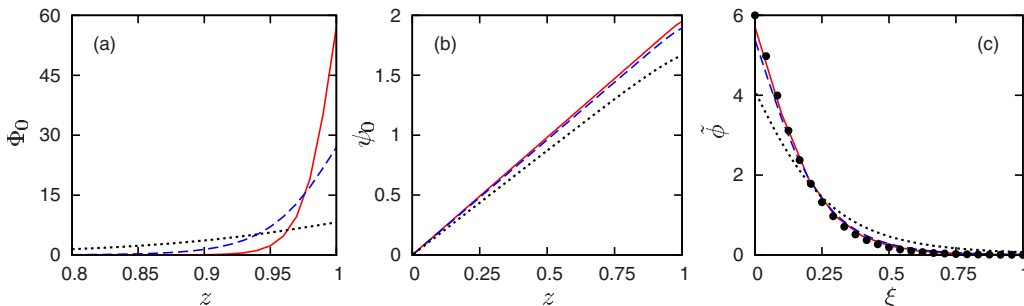


FIG. 2. (Color online) Quasiequilibrium states at $\alpha^2 = 0.5$. Profiles of the concentration of bubbles Φ_0 (a) and velocity potential ψ_0 (b) at $Q_S = 2, 5, 10$, shown by dotted, dashed, and solid lines, respectively. Variation of $\bar{\phi} = Q_S^{-1} \Phi_0$ with $\xi = Q_S(1 - z)$ for the same values of Q_S and α^2 (c); circles represent the asymptotic law according to formula (17).

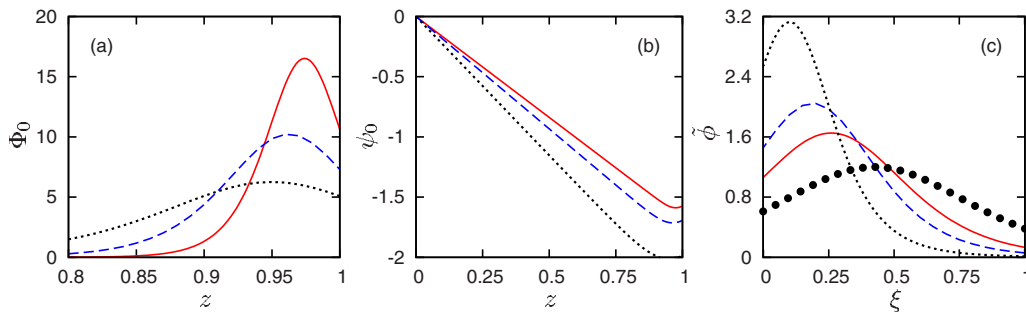


FIG. 3. (Color online) Quasiequilibrium states at $\alpha^2=1.7$. Profiles of the concentration of bubbles Φ_0 (a) and velocity potential ψ_0 (b) at $Q_S=2, 5, 10$, shown by dotted, dashed, and solid lines, respectively. Variation of $\tilde{\phi}=Q_S^{-1}\Phi_0$ with $\xi=Q_S(1-z)$ for the same values of Q_S and α^2 (c); circles represent the asymptotic law according to formula (17).

with $f_0=(4\alpha^2 C_1 \cos^2 \alpha + 3)/(8\alpha^2 \cos^3 \alpha)$.

These results can be easily explained as follows. Small values of Q_S are equivalent to intensive diffusion. As a result, spatial inhomogeneities in the distribution of bubbles are smoothed out by diffusion. The Bjerknes force can lead to a small correction only, which results in a weakly nonuniform concentration field. Note that this quasiequilibrium resembles the solution obtained for early stages of evolution in the nondiffusive approximation [see formulas (71) and (73) in Ref. 14]. This similarity is caused by the initial conditions chosen in the form of uniformly distributed bubbles.¹⁴

We next discuss numerical results. In Fig. 2 we show distributions of Φ_0 and ψ_0 for $\alpha^2=0.5$. The dependencies are presented for different values of Q_S . We note that the potential is linear everywhere, except for the domain in the vicinity of the wall. Because of the exponential dependence of Φ_0 on ψ_0 , even a small change in profile $\psi_0(z)$ drastically influences the concentration profile. To validate asymptotic solution (17) for large Q_S , we provide Fig. 2(c). Here, we demonstrate the variation of the auxiliary field $\tilde{\phi} \equiv Q_S^{-1}\Phi_0$ as a function of ξ . It can be seen that even at $Q_S=5$ the numerical results are in good agreement with the asymptotic solution.

Similar solutions are shown in Fig. 3 for $\alpha^2=1.7$, when the maximum of concentration is close to the wall, but not directly at it. This kind of the concentration pattern has been rigorously confirmed for large Q_S . However, as can be seen in Fig. 3(a), a very similar situation takes place for finite values of Q_S . For the values of Q_S used in Fig. 3, the asymptotic solution is not as good as in the case shown in Fig. 2. It should be emphasized that the reliable agreement with the asymptotic solution is achieved at $Q_S \geq 50$.

The dependence of the concentration maximum on parameter Q_S is demonstrated in Fig. 4. As has been stated earlier, one sees that the smaller the value of α is, the better asymptotic formula (17) works.

In Fig. 5 we plot numerically obtained profiles for larger values of α^2 . For $\alpha^2=4, 16$, and 40 one, two, and three bubbly screens, respectively, exist in half of the layer, $0 \leq z \leq 1$. The velocity potential is nearly a piecewise-linear function of z .

B. High frequencies

At high frequencies, $\Omega < 1$, we introduce another auxiliary parameter

$$\tilde{\alpha}^2 \equiv -\frac{3\Phi_a}{\Omega^2 - 1}$$

and recall that for high frequencies $Q_S < 0$.

In the limiting case $|Q_S| \equiv \varepsilon^{-2} \gg 1$ we obtain

$$\Phi_0 \approx \varepsilon^{-1}\Phi_0^{(0)} + \Phi_0^{(1)}, \quad \Phi_0^{(0)} = \frac{2}{\sqrt{\pi}} \exp(-\tilde{\xi}^2), \quad (25a)$$

$$\Phi_0^{(1)} = \tilde{\alpha}^2 \Phi_0^{(0)} \left(\tilde{\xi} \operatorname{erf} \tilde{\xi} - \frac{1}{\sqrt{2\pi}} \right), \quad (25b)$$

$$\psi_0 = z + \varepsilon^2 g(\tilde{\xi}), \quad g \equiv -\frac{\tilde{\alpha}^2}{2} \operatorname{erf} \tilde{\xi}, \quad (25c)$$

where $\tilde{\xi} \equiv z/\varepsilon$ and $\operatorname{erf} z \equiv (2/\sqrt{\pi}) \int_0^z \exp(-y^2) dy$ is the error function. This solution indicates that the bubbles accumulate at the center of the layer, $z=0$, which corresponds to the node of the pulsation pressure. The velocity potential is the same as for the pure liquid up to a small correction. For instance, the numerically obtained results shown in Fig. 6(a) perfectly match asymptotical solution (25).

In the opposite case, $|Q_S| \ll 1$, the nonuniformity of concentration is small, Φ_0 is weakly enhanced at the center with

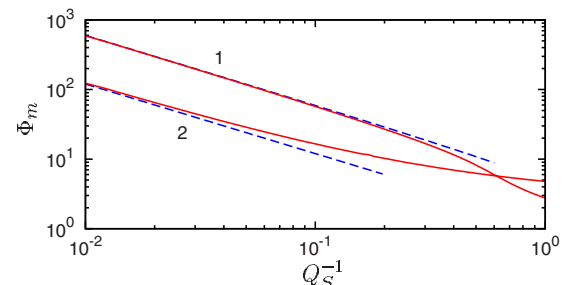


FIG. 4. (Color online) Maximal value of the bubble concentration, $\Phi_m = \max_z \Phi_0(z)$, as a function of Q_S^{-1} . Solid lines show the numerical results; dashed lines are plotted according to formula (17), for $Q_S \rightarrow \infty$. Lines 1 correspond to $\alpha^2=0.5$ and lines 2 correspond to $\alpha^2=1.7$.

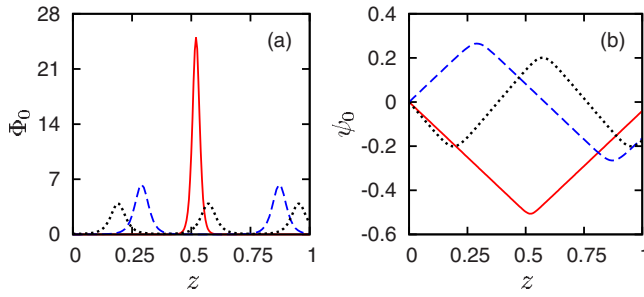


FIG. 5. (Color online) Profiles of the bubble concentration (a) and the potential of the pulsation velocity (b) plotted for $Q_S=100$. Solid, dashed, and dotted lines correspond to $\alpha^2=4, 16, 40$, respectively.

a relative decrease near the boundaries. This case is described by an asymptotic solution of the form

$$\psi_0 = \psi_0^{(0)} + \frac{Q_S}{8\tilde{\alpha}^2 \cosh^3 \tilde{\alpha}} \psi_0^{(1)}, \quad \psi_0^{(0)} = \frac{\sinh \tilde{\alpha} z}{\tilde{\alpha} \cosh \tilde{\alpha}}, \quad (26)$$

$$\Phi_0 = 1 + Q_S(\psi_0^2 + C_1), \quad C_1 = \frac{2\tilde{\alpha} - \sinh 2\tilde{\alpha}}{4\tilde{\alpha}^3 \cosh^2 \tilde{\alpha}}, \quad (27)$$

with

$$\psi_0^{(1)} = \tilde{f}_0[z \cosh \tilde{\alpha} z - (\cosh \tilde{\alpha} - \tilde{\alpha} \sinh \tilde{\alpha}) \psi_0^{(0)}] + \frac{1}{4\tilde{\alpha}}[\sinh 3\tilde{\alpha} z - 3\tilde{\alpha} \cosh 3\tilde{\alpha} \psi_0^{(0)}], \quad (28)$$

where $\tilde{f}_0 = (4\tilde{\alpha}^2 C_1 \cosh^2 \tilde{\alpha} - 3)$.

We point out an interesting case where the frequency of external driving only slightly exceeds the eigenfrequency of a single bubble, which corresponds to high values of $\tilde{\alpha}$. Physically, this means that a boundary layer emerges near the wall and the velocity potential is small beyond this layer. For this reason, we introduce the fast coordinate $\eta \equiv \tilde{\alpha}(1-z)$ and present the velocity potential as

$$\psi_0 = \tilde{\alpha}^{-1} f(\eta). \quad (29)$$

Since the potential ψ_0 is small, we notice from Eq. (12) that the concentration is nearly unity. This observation allows us

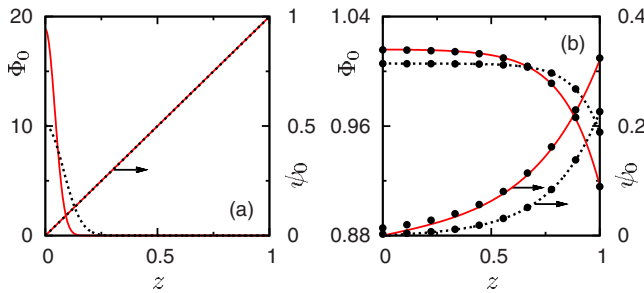


FIG. 6. (Color online) Profiles of the bubble concentration and the velocity potential for different Q_S and $\tilde{\alpha}^2$. The results correspond to $\tilde{\alpha}^2=0.1$, parameter $Q_S=-80$ (dotted lines) and $Q_S=-280$ (solid lines) (a). On the scale of the figure, the solid and dotted lines for the potential ψ_0 cannot be distinguished. Similar dependencies for $Q_S=-1$ (b). Parameter $\tilde{\alpha}^2=10$ (solid lines) and $\tilde{\alpha}^2=20$ (dotted lines). Asymptotical solution (30) valid for large $\tilde{\alpha}^2$ is shown by circles.

to linearize Eq. (14) and to figure out that $f = \exp(-\eta)$. As a result, we obtain

$$\psi_0 = \tilde{\alpha}^{-1} e^{-\eta} + \frac{Q_S}{8\tilde{\alpha}^3} (e^{-3\eta} - 3e^{-\eta}), \quad (30a)$$

$$\Phi_0 = 1 + \frac{Q_S}{\tilde{\alpha}^2} e^{-2\eta} - \frac{Q_S}{2\tilde{\alpha}^3}. \quad (30b)$$

The comparison of result (30) with the numerical solution is provided in Fig. 6(b). It is clearly seen that the asymptotic solution works well even at $\tilde{\alpha}^2=20$. With the increase of $|Q_S|$, the difference between the analytical and numerical results becomes more pronounced. This tendency is clearly seen from expression (30b). Larger values of $|Q_S|$ mean stronger influence of the nonuniform part of concentration.

IV. STABILITY ANALYSIS

We now pose the question whether the solutions found in Sec. III are stable. To answer this question, we introduce small perturbations of the bubble concentration ϕ , velocity potential of the pulsation motion Ψ , liquid velocity \mathbf{U} , and pressure P . By substituting the perturbed fields into Eqs. (5) and (6) and linearizing the problem with respect to small perturbations, we arrive at

$$\frac{1}{S} \frac{\partial \mathbf{U}}{\partial t} = -\nabla P + \nabla^2 \mathbf{U} + 3\Phi_a \mathbf{F}, \quad \text{div } \mathbf{U} = 0, \quad (31a)$$

$$\frac{\partial \phi}{\partial t} = -\mathbf{U} \cdot \nabla \Phi_0 - \text{div } \mathbf{J}, \quad \mathbf{J} \equiv \mathbf{F} - \nabla \phi, \quad (31b)$$

$$\mathbf{F} = Q_S [2\Phi_0 \nabla (\psi_0 \Psi) + \phi \nabla \psi_0^2], \quad (31c)$$

$$\nabla^2 \Psi = -\frac{3\Phi_a}{\Omega^2 - 1} (\Phi_0 \Psi + \psi_0 \phi), \quad (31d)$$

$$z = \pm 1: \quad \mathbf{U} = \mathbf{e}_z \cdot \mathbf{J} = \mathbf{e}_z \cdot \nabla \Psi = 0. \quad (31e)$$

Since the base quasiequilibrium state possesses O_2 symmetry, we do not have to treat the full three-dimensional stability problem. For this reason, we restrict our analysis by the two-dimensional consideration. We assume that all the perturbation fields are independent of y and the corresponding component of the velocity vanishes, $U_y=0$. As a result, for the two-dimensional incompressible velocity field we can introduce a streamfunction φ defined by a relation

$$\mathbf{U} = \nabla \times (\varphi \mathbf{e}_y), \quad (32)$$

where $\mathbf{e}_y = (0, 1, 0)$.

We apply the operation of $\nabla \times$ to Eq. (31a) and consider the perturbations proportional to $\exp(ikx + \lambda t)$. Here k is the real wave number and λ is the complex growth rate. As a result, we obtain a boundary value problem for the z -dependent amplitudes of the perturbations

$$\frac{\lambda}{S} \hat{D}^2 \varphi = \hat{D}^4 \varphi - 6ikQ_S \Phi_a \Psi_0 (\Phi_0' \Psi - \psi_0' \phi), \quad (33a)$$

$$\lambda \phi = -ik\Phi_0' \varphi - J' + k^2(2Q_S \Phi_0 \psi_0 \Psi - \phi), \quad (33b)$$

$$\hat{D}^2 \Psi = -\frac{3\Phi_a}{\Omega^2 - 1} (\Phi_0 \Psi + \psi_0 \phi), \quad (33c)$$

$$z = \pm 1: \quad \varphi = \varphi' = J = \Psi' = 0, \quad (33d)$$

where $\hat{D}^2 = d^2/dz^2 - k^2$ is the Fourier image of the Laplace operator and

$$J \equiv 2Q_S[\Phi_0(\psi_0 \Psi)' + \psi_0 \psi_0' \phi] - \phi'.$$

Having solved this boundary value problem, one finds the spectrum of eigenvalues λ as a function of dimensionless parameters. The analytical solution can be obtained only in a few limiting cases. To solve the problem numerically, we apply the conventional shooting method. We note that in all our calculations λ is found to be real.

We emphasize that to consider a practically relevant limit of large Schmidt numbers, $S \gg 1$, one should suppress the left hand side of Eq. (33a), which simplifies the analysis. Physically, this approximation implies a very fast relaxation of the perturbations associated with the flow.

A. Low frequencies

It can be easily shown that the quasiequilibrium state is unstable for $\Omega > 1$ at arbitrarily small Q_S . To prove this statement, let us look at the stability problem in the limit of small external driving, $Q_S \ll 1$, when the base state is defined by Eq. (23). For the sake of brevity, below we omit superscript “(0)” for the leading part of the potential $\psi_0^{(0)}$. Any confusion is unlikely because the first correction $\psi_0^{(1)}$ does not influence the further analysis. We expand the perturbations and the growth rate λ in series with respect to Q_S ,

$$\phi = \phi_0 + Q_S \phi_1 + \dots, \quad \Psi = \Psi_0 + Q_S \Psi_1 + \dots, \quad (34a)$$

$$\varphi = \varphi_0 + Q_S \varphi_1 + \dots, \quad (34b)$$

and to the zeroth order arrive at the problem

$$\hat{L}_\varphi \varphi_0 \equiv \hat{D}^2(\hat{D}^2 - \lambda S^{-1})\varphi_0 = 0, \quad (35a)$$

$$\hat{L}_\phi \phi_0 \equiv (\hat{D}^2 - \lambda)\phi_0 = 0, \quad (35b)$$

$$\Psi_0'' = (k^2 - \alpha^2)\Psi_0, \quad (35c)$$

$$z = \pm 1: \quad \varphi_0 = \varphi_0' = \phi_0' = \Psi_0' = 0. \quad (35d)$$

As we see, all the fields are decoupled, the solutions for φ_0 and ϕ_0 are given by sets of even and odd functions with real negative eigenvalues λ . Note that the eigenvalues associated with φ_0 are proportional to the Schmidt number. As S is large for real bubbly liquids, the perturbations of the flow decay extremely fast. The eigenvalue spectrum of the concentration, which is used in the further argumentation, is given by values

$$\lambda_n = -\left(k^2 + \frac{n^2 \pi^2}{4}\right), \quad n = 0, 1, 2, \dots \quad (36)$$

In other words, all the mentioned modes are decaying in time and therefore cannot lead to instability. Now we are interested in growing and neutrally stable modes ($\lambda \geq 0$) and to this order we should set

$$\varphi_0 = 0, \quad \phi_0 = 0. \quad (37)$$

The solution for the velocity potential is trivial, $\Psi_0 = 0$, unless $k = \sqrt{\alpha^2 - \pi^2 m^2/4}$, $m = 0, 1, \dots$. We next deal with the simplest case of $m = 0$, which is the only option allowed for all possible α . In this case the boundary value problem for Ψ_0 has a constant solution, which can be set to unity without loss of generality,

$$\Psi_0 = 1. \quad (38)$$

As we see, to the zeroth order no instability is detected and we proceed to the next order. Thus, in addition to expansions (34) we present the wave number as

$$k = \alpha + Q_S k_1 + \dots \quad (39)$$

and to the first order in Q_S we obtain the problem

$$\hat{L}_\varphi \varphi_1 = 0, \quad (40a)$$

$$\hat{L}_\phi \phi_1 = 2(\psi_0'' - \alpha^2 \psi_0)\Psi_0, \quad (40b)$$

$$\Psi_1'' = [2\alpha k_1 - \alpha^2 \Phi_0^{(1)}]\Psi_0 - \alpha^2 \psi_0 \phi_1, \quad (40c)$$

$$z = \pm 1: \quad \varphi_1 = \varphi_1' = \Psi_1' = 0, \quad \phi_1' = 2\Psi_0. \quad (40d)$$

The solution for the streamfunction $\varphi_1 = 0$ as before, whereas for the concentration of bubbles we obtain either

$$\phi_1 = \frac{2}{2\alpha^2 + \lambda} \left(2\alpha^2 \psi_0 + \lambda \frac{\sinh qz}{q \cosh q} \right), \quad \lambda > -\alpha^2, \quad (41)$$

or

$$\phi_1 = \frac{2}{2\alpha^2 + \lambda} \left(2\alpha^2 \psi_0 + \lambda \frac{\sin \tilde{q}z}{\tilde{q} \cos \tilde{q}} \right), \quad \lambda < -\alpha^2, \quad (42)$$

where $q^2 = \alpha^2 + \lambda$ and $\tilde{q}^2 = -\alpha^2 - \lambda$. As it can be seen from relation (36) for $k = \alpha$, solution (42) diverges at $\lambda = \lambda_n$ for n odd.

The solvability condition for Eq. (40c) with appropriate boundary conditions can be obtained by integrating this equation across the layer, which for $\lambda > -\alpha^2$ yields

$$k_1 = k_{qe} + \lambda \frac{q \sin \alpha \cosh q - \alpha \cos \alpha \sinh q}{(2\alpha^2 + \lambda)^2 q \cos \alpha \cosh q}, \quad (43)$$

and in the opposite case, $\lambda < -\alpha^2$ we have

$$k_1 = k_{qe} - \lambda \frac{\tilde{q} \sin \alpha \cos \tilde{q} - \alpha \cos \alpha \sin \tilde{q}}{(2\alpha^2 + \lambda)^2 \tilde{q} \cos \alpha \cos \tilde{q}}, \quad (44)$$

where

$$k_{qe} \equiv \frac{2\alpha - \sin 2\alpha}{2(2\alpha^2 + \lambda) \cos^2 \alpha} > 0. \quad (45)$$

The condition of neutral stability is defined by the requirement $\lambda = 0$, which leads to $k_1 = k_{qe}|_{\lambda=0} \equiv k_{qe}(0)$. Taking this

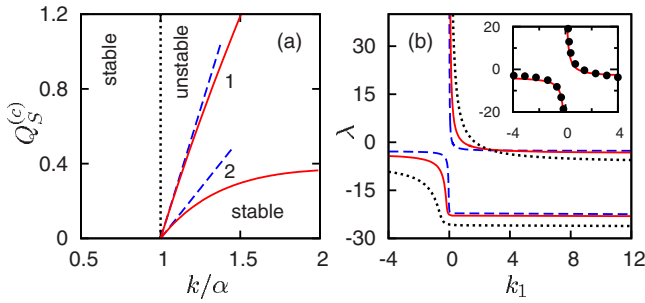


FIG. 7. (Color online) Stability diagram (a) for $\alpha^2=0.1$ (lines 1) and $\alpha^2=1$ (lines 2). Solid and dashed lines correspond to numerical calculations and analytical result (46), respectively. Growth rates λ as functions of k_1 (b). Dashed, solid, and dotted lines present the dependence at $\alpha^2=0.25, 1, 4$, respectively. The inset provides the comparison of numerical results (circles) and analytical solutions (43) and (44) (solid lines) for $Q_S=0.2$ and $\alpha^2=1$.

observation into account in relation (39) we figure out the border of stability to be

$$Q_S^{(c)} = \frac{k - \alpha}{k_{qe}(0)}, \quad (46)$$

which is valid at small Q_S and $k \approx \alpha$. This result is in good agreement with the numerical calculations, see Fig. 7. We indicate that the stability border is independent of both Φ_a and S , even for finite Q_S . As we see, perturbations grow at any $Q_S > Q_S^{(c)}$. This growth takes place even for infinitely small intensity of external driving, where the perturbations are characterized by k slightly exceeding α . As a result, we conclude that at low frequencies, $\Omega > 1$, the quasiequilibrium state is *always unstable*.

Let us go back to small values of Q_S . We note that by setting $\lambda=0$ in Eq. (41), one ends up with $\phi_1=2\psi_0$. For the full concentration field we have [see relations (23)]

$$\begin{aligned} \Phi &\approx \Phi_0 + Q_S \phi_1 \\ &\approx C \exp[Q_S(\psi_0 + \Psi_0)^2] \\ &\approx 1 + Q_S(\psi_0^2 + C_1) + 2Q_S\psi_0\Psi_0. \end{aligned} \quad (47)$$

This fact indicates that for small Q_S solution (12) remains valid even for the perturbed fields taken at the stability border, $k_1=k_{qe}(0)$, with $\Phi=\Phi_0+Q_S\phi_1$ and $\psi=\psi_0+\Psi_0$ instead of Φ_0 and ψ_0 , respectively. Hence, the branching solution is another quasiequilibrium state, but in contrast to that one in Sec. III this state is two dimensional. This is a direct consequence of the specific form of function Φ . With the concentration being an arbitrary function of potential ψ and the potential only, $\Phi=F(\psi)$, the feedback term in Eq. (5a) can always be presented as gradient. Thus, this term redistributes pressure but does not generate the averaged liquid flow. Note that this result is valid even at finite values of $k-\alpha$ and explains why the stability border is independent of S and Φ_a for α fixed. These parameters enter Eqs. (5) and (6) only together with \mathbf{u} .

Let us now discuss the behavior of the growth rates as functions of k . At $k \approx \alpha$ these dependencies are described by Eqs. (43) and (44), which are tabulated in Fig. 7(b). The inset of this figure provides a comparison with the numerically obtained results. It can be seen that k_1 tends to infinity as

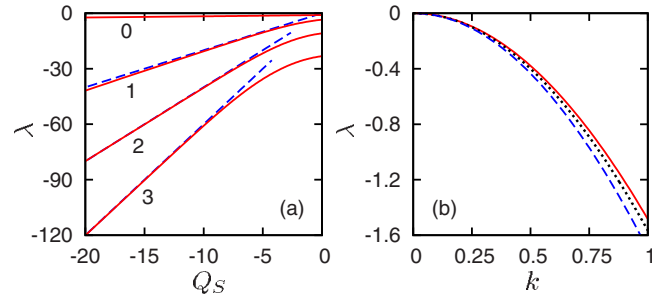


FIG. 8. (Color online) Growth rates at high frequencies plotted for $\bar{\alpha}^2=0.1$, $S=100$, $\Phi_a=1$. Four lower branches of the spectrum at $k=1$, where solid lines present numerical results and dashed lines show the approximation for $|Q_S| \gg 1$, see formula (48) for $n=1, 2, 3$ (a). Variation of the growth rate with k for $Q_S=-100$ (solid line) and $Q_S=-280$ (dotted line); dashed line shows the asymptotic law according to formula (49) (b).

$\lambda \rightarrow \lambda_n$ for n odd, see relation (36). This result is reasonable as it provides the matching of the different solutions separated by the critical value $k=\alpha$. Next, it is clear from Fig. 7(b) that in the vicinity of $k=\alpha$ a rearrangement of branches occurs. Starting from λ_n with n odd at $k > \alpha$, the growth rate steadily increases with the decrease in k and at $k < \alpha$ reaches the value λ_{n-2} . Moreover, a similar variation of the lowest odd branch, namely, λ_1 , results in $\lambda \rightarrow +\infty$ as $k \rightarrow \alpha+0$. Thus, the growth rate has a pole at $k=\alpha$ and no positive growth rates exist in the spectrum at $k < \alpha$. For this reason, the domain with $k < \alpha$ is marked as “stable” in Fig. 7(a).

This unstable mode originates from the problem of natural oscillations for the velocity potential ψ (for the uniform distribution of bubbles), $\Phi_0=1$. As we see from Eq. (40b), this eigenmode induces the perturbations of concentration. Because of feedback, the bubble concentration influences the potential and the system eventually becomes unstable. This instability takes place for a base state with any nonvanishing ψ_0 . The simplest example of such mode, inherent in Eqs. (5) and (6), is analyzed in Appendix A.

B. High frequencies

We now consider the stability at high frequencies, $\Omega < 1$. As well as in a few limiting cases observed earlier, boundary value problem (33) admits an analytical solution.

First, we focus on the limit of large $|Q_S|$, when the bubbles accumulate at the center of the layer and the potential of pulsation motion is nearly linear. This base state is described by Eq. (25). An accurate analysis of this situation is performed by the method of matched expansions (see Appendix B), which results in the spectrum of growth rates

$$\lambda_n = 2nQ_S, \quad n = 0, 1, 2, \dots \quad (48)$$

Numerical results and asymptotic law (48) agree well. The agreement becomes better for bigger n , see Fig. 8(a).

Except for $n=0$, these branches display strong temporal decay of perturbations, which increases with the growth of the driving intensity, $|Q_S|$. Quite a similar behavior of the spectrum has been recently observed for dielectric particles accumulated at the center of the layer under the action of dielectrophoretic force.¹⁵

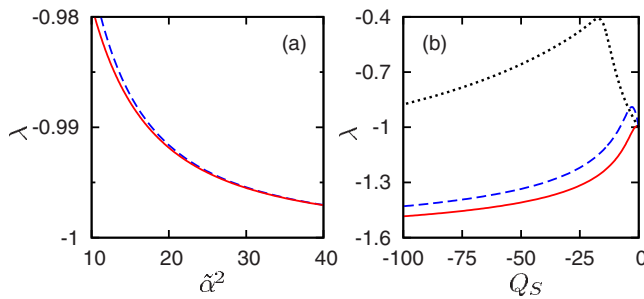


FIG. 9. (Color online) Growth rates at high frequencies presented for $S = 100$, $\Phi_a = 1$, and $k = 1$. Comparison of numerical data (solid line) and approximate formula (50) (dashed line), $Q_S = -1$ (a). Variation of the growth rates with Q_S ; parameter $\tilde{\alpha}^2 = 0.1, 1, 10$ correspond to solid, dashed, and dotted lines, respectively (b).

For $n=0$ a more delicate analysis is needed. Referring to Appendix B for the details, we provide here the eventual result valid at the limit $S \gg 1$,

$$\lambda_0 = -k^2 - 3\Phi_a k \frac{\sinh^2 k - k^2}{\sinh 2k - 2k} + O\left(\frac{1}{\sqrt{|Q_S|}}\right). \quad (49)$$

Figure 8(b) shows the comparison of numerical results with approximation (49). Again, the results agree well, although with a slight distinction for higher k , where the correction to λ_0 becomes non-negligible.

In another limiting case, $\tilde{\alpha}^2 \gg 1$, when the base state is given by Eq. (30), the largest growth rate is

$$\lambda = -k^2 \left(1 + \frac{3Q_S}{4\tilde{\alpha}^3}\right). \quad (50)$$

Note that the Bjerknes force provides a small *negative* correction to the decay rate caused by diffusivity so that the role of vibration force is destabilizing. As becomes evident from Fig. 9(a), formula (50) works well even at $\tilde{\alpha}^2 = 10$.

We have also checked several other limiting cases: $\Phi_a \ll 1$, when there is no generation of the averaged flow, and $\tilde{\alpha}^2 \ll 1$, when the potential of the pulsation motion is linear. These analyses as well as numerical tests show that quasiequilibrium state is stable. An example of calculations in which the Bjerknes force may become destabilizing is presented in Fig. 9(b). This destabilization, however, does not eventually lead to instability. Thus, our numerical and analytical results show that at high frequency the quasiequilibrium state is stable.

V. CONCLUSIONS

We have considered the dynamics of monodisperse bubbly liquid confined by the plane solid walls. The system is subject to small-amplitude high-frequency transverse harmonic oscillations. The period of these oscillations is assumed to be small in comparison with typical relaxation times for a single bubble. At the same time, the ratio Ω of the eigenfrequency of volume oscillations to the frequency of external driving is of order unity. The time-averaged description developed in Ref. 14 has been generalized. In contrast to the original model, we have taken into account the *diffusivity* of bubbles, which allows us to prevent unbounded accumu-

lation of bubbles found out earlier.¹⁴ As we have demonstrated, a possible mechanism leading to the spatial diffusivity of bubbles can be associated with a slight imperfection of the experimental setup, where the imposed oscillations are assumed to be not perfectly harmonic and transverse.

The *quasiequilibrium states*, in which the liquid is quiescent on average and the concentration of bubbles is non-uniform, have been systematically explored. In the state of quasiequilibrium, the Bjerknes force, which acts on *compressible bubbles*, is balanced by the diffusive flux of bubbles. We stress that in contrast to the case of a single bubble, the ensemble of bubbles significantly influences the characteristics of the liquid phase, which is referred to as *feedback effects*. Technically, this collective bubbly ensemble-induced effect is taken into account by retaining the two-way coupling between the liquid and the bubbles. As a result, we are able to observe that the bubbles influence the pulsation field and therefore the Bjerknes force itself is changed.

At a *low frequency*, $\Omega > 1$, we detect accumulation of bubbles either at the solid boundaries or in planes parallel to the walls. The bubbly screens predicted in nondiffusive consideration¹⁴ are now smeared by diffusion. As a result, the corresponding structures are stationary and are no longer singular objects. We have shown that all these one-dimensional states turn out to be unstable. Interestingly, the branching solution satisfies the criterion of quasiequilibrium. This fact indicates that although the one-dimensional solutions are unstable, two-dimensional quasiequilibrium states and their stability may become of interest.

At a *high frequency*, $\Omega < 1$, the maximal value of the concentration is at the center plane of the system. As in the case of low frequencies, when the Bjerknes force dominates over the diffusive flux, this peak can be very sharp or smooth in the opposite case. This one-dimensional state has been shown to be stable for any values of governing parameters.

Finally, we stress that our study has been based on the model full in the sense that it generally admits the existence of averaged flow, see Eqs. (5) and (6). We have arrived at the conclusion that the quasiequilibrium state does take place and no generation of the averaged flow occurs. This is in contrast to the previous studies,^{10–13} where a reduced description neglecting the possibility of the averaged flows is accepted *a priori*, as an approximation. Furthermore, we have performed the stability analysis, where the nonvanishing perturbations associated with the averaged flow are retained. These perturbations turn out to be especially important for the case of high frequency, $\Omega < 1$, see Sec. IV B.

ACKNOWLEDGMENTS

We are grateful to D. S. Goldobin for fruitful discussions. S.S. thanks the Foundation “Perm Hydrodynamics” for partial support, A.S. was supported by German Science Foundation, DFG SPP 1164 “Nano- and microfluidics,” Project No. 1021/1-2. This research has been recognized by German Science Foundation (DFG) and Russian Foundation for Basic Research (RFBR) as a joint German-Russian collaborative initiative (DFG Project No. 436 RUS113/977/0-1

and RFBR Project No. 08-01-91959). The authors gratefully acknowledge the funding organizations for support.

APPENDIX A: STABILITY OF UNIFORM OSCILLATIONS OF BUBBLY LIQUID

Consider motionless bubbly liquid, $\mathbf{u}_0=0$, which occupies infinite space. We assume that bubbles are uniformly distributed, $\Phi_0=1$, and admit that $\psi_0=1$. Recall that while obtaining the averaged model,¹⁴ the pressure pulsations were assumed proportional to the velocity potential, ψ . Hence, physically, the assumption of $\psi_0=1$ implies spatially uniform oscillations of the pressure field. We indicate that although from the practical point of view this assumption is rather hypothetical, it helps us to figure out the reason for the instability found in Sec. IV A. Thus, in the system under consideration, the pressure oscillates with an amplitude Π and frequency ω , low in the sense $\Omega > 1$. For this system, the parameter characterizing external driving is $Q_S = \Pi^2(2\rho\omega)^{-2}[\nu D(\Omega^2 - 1)]^{-1}$.

In order to investigate the stability of this state, we introduce small perturbations of the concentration, ϕ , and the potential of the pulsations, Ψ . After the linearization of Eqs. (5) and (6) with respect to the perturbations, one arrives at the problem

$$\frac{\partial \phi}{\partial t} + 2Q_S \nabla^2 \Psi = \nabla^2 \phi, \quad (\text{A1a})$$

$$\nabla^2 \Psi + \alpha^2(\phi + \Psi) = 0. \quad (\text{A1b})$$

We note that the perturbations of the velocity effectively decouple and turn out to decay. This is so because for the case of interest the averaged vibration force in Eq. (5a) becomes gradient. Hence no averaged flow can be induced within the linear approximation.

We seek the solution of Eq. (A1) proportional to $\exp(\lambda t + i\mathbf{k} \cdot \mathbf{r})$ and obtain a dispersion relation

$$\lambda = -k^2 - \frac{2Q_S k^2 \alpha^2}{\alpha^2 - k^2}, \quad (\text{A2})$$

where k is the wave number.

This relation qualitatively reproduces the picture of the instability shown in Fig. 7(b). As we can see, λ is positive in the range $\alpha < k < k_c$, where $k_c^2 = \alpha^2(1 + 2Q_S)$, with $\lambda \rightarrow +\infty$ as $k \rightarrow \alpha + 0$. On the other hand, λ is negative and therefore no instability takes place at $k < \alpha$.

Thus, this simplified analysis shows clearly that the instability found in Sec. IV A is generic. This kind of instability is not a feature of the particular problem, it arises for any nontrivial distribution of the pulsation potential ψ_0 .

APPENDIX B: STABILITY OF QUASIEQUILIBRIUM IN THE LIMIT OF LARGE NEGATIVE Q_S

To study the stability of the quasiequilibrium state at large $|Q_S|$ we apply the method of matched expansions. We introduce the fast coordinate $\xi = z/\varepsilon$. As we have done earlier, $\varepsilon^{-1} = \sqrt{|Q_S|}$, for the sake of brevity we suppress tilde for $\tilde{\xi}$. The solution of the inner problem depends on ξ , and is sought in the form

$$\phi^{(i)} = \phi_0 + \varepsilon \phi_1 + \varepsilon^2 \phi_2 + \dots, \quad (\text{B1})$$

$$\varphi^{(i)} = \varepsilon^2(\varphi_0^{(i)} + \varphi_1^{(i)} + \dots), \quad (\text{B2})$$

$$\Psi^{(i)} = \varepsilon^3(\Psi_0^{(i)} + \dots). \quad (\text{B3})$$

The solution of the outer problem, which depends on z , is presented as

$$\phi^{(o)} = e.s.t., \quad (\text{B4})$$

$$\varphi^{(o)} = \varepsilon(\varphi_0^{(o)} + \dots), \quad \Psi^{(o)} = \varepsilon^3(\Psi_0^{(o)} + \dots). \quad (\text{B5})$$

Here, *e.s.t.* is used to denote exponentially small terms. Since $\phi^{(o)}$ is negligibly small, we omit the superscripts for $\phi_j^{(i)}$, $j=0, 1, 2, \dots$

Next, we assume that the growth rate is large in the sense

$$\lambda = \varepsilon^{-2} \Lambda \quad (\text{B6})$$

and also take into account the power expansions of Φ_0 and ψ_0 given by relation (25) with respect to ε . As a result, we obtain

$$\phi_{0\xi\xi} + 2(\xi\phi_0)_\xi - \Lambda\phi_0 = 0, \quad (\text{B7a})$$

$$d_\xi^4 \varphi_0^{(i)} = 0, \quad (\text{B7b})$$

$$\Psi_{0\xi\xi} - \tilde{\alpha}^2 \xi \phi_0 = 0, \quad (\text{B7c})$$

where subscript ξ is applied to denote the derivative with respect to ξ .

By means of the ansatz $\phi_0 = \tilde{\phi}_0 \exp(-\xi^2)$, Eq. (B7a) is reduced to Hermite's equation

$$\tilde{\phi}_{0\xi\xi} - 2\xi\tilde{\phi}_{0\xi} - \Lambda\tilde{\phi}_0 = 0, \quad (\text{B8})$$

which for $\Lambda_n = -2n$, $n=0, 1, 2, \dots$ admits the solution given by the Hermite polynomials. Other possible values of Λ and the corresponding solutions are out of interest because no proper matching with the outer problem can be achieved.

Accounting for the rescaling of the growth rate [see relation (B6)], we end up with result (48) for the spectrum of growth rates. The solutions with $n > 0$ describe very fast temporal decay of perturbations. Hence, the only case that should be analyzed separately corresponds to $n = \Lambda_0 = 0$, when $\lambda = O(1)$. In this case, the solution of Eq. (B7a) is as follows:

$$\phi_0 = \frac{2}{\sqrt{\pi}} e^{-\xi^2}, \quad (\text{B9})$$

so that ϕ_0 coincides with $\Phi_0^{(0)}$, cf. Eq. (25a).

Solutions of Eqs. (B7b) and (B7c) are given by

$$\varphi_0^{(i)} = B_1 \xi + B_3 \xi^3, \quad \Psi_0^{(i)} = g(\xi), \quad (\text{B10})$$

where B_1 and B_3 are constants and $g(\xi)$ is as in Eq. (25c). Note that because of symmetry, the quadratic and constant terms with respect to ξ are vanishing in the solution for the streamfunction.

To the first order we obtain

$$\phi_{1\xi\xi} + 2(\xi\phi_1)_\xi = -2[\Phi_0^{(0)}(\xi\Psi_0)_\xi + (\xi g)_\xi \varphi_0]_\xi, \quad (\text{B11a})$$

$$d_\xi^4 \varphi_1^{(i)} = 6ik\Phi_a \xi \phi_0, \quad (\text{B11b})$$

and to the second order we arrive at

$$\phi_{2\xi\xi} + 2(\xi\phi_2)_\xi = F_\xi + (\lambda + k^2)\phi_0 + ik\varphi_0\Phi_{0\xi}^{(0)}\xi, \quad (\text{B12})$$

where F is the term unimportant for the further analysis. This term includes the first order corrections to $\Psi^{(i)}$ and the second order corrections to the base state. The first order correction to the potential as well as the second order of the streamfunction is not needed below.

The solvability condition for Eq. (B11a) can be obtained by integrating the equation over ξ from zero to infinity. It can be easily shown that this equation is solvable. Its solution is not used below and therefore is not provided here. A similar condition for Eq. (B12) leads to the relation

$$\lambda + k^2 - ikB_1 + ikB_3 \int_0^\infty \xi^3 \Phi_0^{(0)} d\xi = 0. \quad (\text{B13})$$

The constants B_1 and B_3 included in Eq. (B13) should be found by means of the matching procedure. The correction to the streamfunction is given by

$$\varphi_1^{(i)} = \frac{6ik\Phi_a}{\alpha^2} \int_0^\xi d\eta \int_0^\eta g(\vartheta) d\vartheta. \quad (\text{B14})$$

Keeping in mind the behavior of $g(\xi)$ at large ξ , one obtains the asymptotic law

$$\xi \rightarrow \infty: \quad \varphi_1^{(i)} \rightarrow -\frac{3ik\Phi_a}{2} \xi^2. \quad (\text{B15})$$

Hence, the solution of the inner problem for the streamfunction at large ξ is

$$\begin{aligned} \varphi^{(i)} &\approx \varepsilon^2 (B_1 \xi + B_3 \xi^3) - \varepsilon^3 \frac{3ik\Phi_a}{2} \xi^2 \\ &= \varepsilon^{-1} B_3 z^3 + \varepsilon \left(B_1 z - \frac{3ik\Phi_a}{2} z^2 \right). \end{aligned} \quad (\text{B16})$$

This solution must be matched with the solution of the outer problem

$$\hat{D}^2 (\hat{D}^2 \varphi_0^{(o)} - \lambda \varphi_0^{(o)}) = 0 \quad (\text{B17})$$

with the no-slip condition at $z=1$. Since the perturbations of the concentration are exponentially small in the bulk, no external force acts on the liquid in this domain. The solution of

Eq. (B17) that satisfies the boundary conditions at $z=1$ is

$$\begin{aligned} \varphi_0^{(i)} &= C_1 \left(\frac{\sinh kz_1}{k} - \frac{\sinh qz_1}{q} \right) \\ &\quad + C_2 (\cosh kz_1 - \cosh qz_1), \end{aligned} \quad (\text{B18})$$

where $z_1 \equiv 1-z$ and $q^2 = k^2 + \lambda S^{-1}$. By expanding this solution near $z=0$ and equating the coefficients at equal powers of z with those in Eq. (B16), we find that

$$B_1 = 3ik\Phi_a \frac{q_+^2 \sinh k \sinh q - 2kq(\cosh k \cosh q - 1)}{q_-^2 (q \cosh q \sinh k - k \cosh k \sinh q)}, \quad (\text{B19})$$

with $q_\pm^2 \equiv q^2 \pm k^2$ and $B_3=0$.

Bearing in mind that q and q_\pm depend on λ , we substitute these constants into Eq. (B13) and obtain a transcendent equation with respect to λ . In the practically relevant case of $S \gg 1$, it is necessary to expand q near k , which results in Eq. (49). Note that this approximation works well already at $S=100$, see Fig. 8(b). More precisely, the line corresponding to formula (49) cannot be distinguished from the numerical results based on the solution of Eqs. (B13) and (B19).

¹V. F. K. Bjerknes, *Fields of Force* (Columbia University Press, New York, 1906).

²F. G. Blake, "Bjerknes forces in stationary sound fields," *J. Acoust. Soc. Am.* **21**, 551 (1949).

³A. Eller, "Force on a bubble in a standing acoustic wave," *J. Acoust. Soc. Am.* **43**, 170 (1968).

⁴L. Rayleigh, "On the pressure developed in a liquid during the collapse of a spherical void," *Philos. Mag.* **34**, 94 (1917).

⁵M. Minnaert, "On musical air bubbles and the sounds of running water," *Philos. Mag.* **16**, 235 (1933).

⁶R. F. Ganiev and V. F. Laphchinsky, *Problems of Mechanics in Cosmic Technology* (Mashinostroenie, Moscow, 1978) (in Russian).

⁷L. van Wijngaarden, "One-dimensional flow of liquids containing small gas bubbles," *Annu. Rev. Fluid Mech.* **4**, 369 (1972).

⁸R. E. Caffisch, M. J. Miksis, G. C. Papanicolaou, and L. Ting, "Effective equations for wave propagation in bubbly liquids," *J. Fluid Mech.* **153**, 259 (1985).

⁹E. L. Carstensen and L. L. Foldy, "Propagation of sound through a liquid containing bubbles," *J. Acoust. Soc. Am.* **19**, 481 (1947).

¹⁰Yu. A. Kobelev and L. A. Ostrovsky, "Nonlinear acoustic phenomena due to bubble drift in a gas-liquid mixture," *J. Acoust. Soc. Am.* **85**, 621 (1989).

¹¹I. Akhatov, U. Parlitz, and W. Lauterborn, "Pattern formation in acoustic cavitation," *J. Acoust. Soc. Am.* **96**, 3627 (1994).

¹²U. Parlitz, C. Scheffczyk, I. Akhatov, and W. Lauterborn, "Structure formation in cavitation bubble fields," *Chaos, Solitons Fractals* **5**, 1881 (1995).

¹³I. Akhatov, U. Parlitz, and W. Lauterborn, "Towards a theory of self-organization phenomena in bubble-liquid mixtures," *Phys. Rev. E* **54**, 4990 (1996).

¹⁴A. V. Straube, D. V. Lyubimov, and S. V. Shklyaev, "Averaged dynamics of two-phase media in a vibration field," *Phys. Fluids* **18**, 053303 (2006).

¹⁵S. V. Shklyaev and A. V. Straube, "Particle entrapment in a fluid suspension as a feedback effect," *New J. Phys.* **10**, 063030 (2008).

¹⁶C. W. Gardiner, *Handbook of Stochastic Methods: For Physics, Chemistry and the Natural Sciences* (Springer, Berlin, 2004).

¹⁷V. G. Kozlov, A. A. Ivanova, and P. Evesque, "Sand behavior in a cavity with incompressible liquid under vertical vibrations," *Europhys. Lett.* **42**, 413 (1998).